International Journal of Recent Technology and Engineering (IJRTE)
ISSN: 2277-3878, Volume-8 Issue-3, September 2019

Effect of Viscous Dissipation on MHD Williamson Nanofluid Flow in a Porous Medium

N. Manjula, K. Govardhan, M. N. Rajashekar

Abstract: ***The main objective of this paper is to focus on a numerical study of viscous dissipation effect on the steady state flow of MHD Williamson nanofluid. A mathematical modeled which resembles the physical flow problem has been developed. By using an appropriate transformation, we converted the system of dimensional PDEs (nonlinear) into coupled dimensionless ODEs. The numerical solution of these modeled ordinary differential equations (ODEs) is achieved by utilizing shooting technique together with Adams-Bashforth Moulton method of order four. Finally, the results of discussed for different parameters through graphs and tables.***

Keyword: Williamson Nanofluid, Adams – Moulton method; Thermophoresis; Brownian motion; viscous dissipation nanofluids.

I. INTRODUCTION

A substance in the gas or liquid phase is referred to as the fluid. Flow of fluid has all kinds of aspects, steady and unsteady, compressible and incompressible, viscous and inviscid, rotational and irrotational, uniform and non-uniform etc.,Meir [1]. The study of fluid flow on a stretching surface is one of the important problems in the current era, as it occurs in different processes of engineering for example, extrusion, wire drawing, food manufacturing, metal spinning, manufacturing of rubber sheets and cooling of huge metallic plates such as an electrolyte, etc. Sakiadis [2] was the first who introduced the problem of boundary layer approximations over stretching surface. The flow caused by stretching sheet was investigated by Crane [3]. Recently, many researchers such as Shehzad et al. [4],Zheng et al. [5], and Gireesha et al. [6] due to wide applications as described above.

The study of magnetic properties of electrically conducting fluids is known as Magnetohydrodynamics (MHD). MHD fluid flow was first introduced by Swedish Physicist, Alfven [7]. In recent years, mass and heat transfer on unsteady MHD natural convention rotating flow of fluid about a porous plate with heat transfer and radiation was studied by Mbeledogu and Ogulu [8]. Kesavaiah et al. [9] investigated the unsteady MHD convective flow over a vertical porous plate. The Jeffrey fluid effect of convection in MHD flow of heat transfer about a stretching sheet is reported by Hayat et al. [10]. Mustafa et al. [11] inspected the MHD Maxwell fluid flow with convective heat transfer. MHD viscous incompressible flow has many applications in engineering for example, cooling of reactors, a power generator, MHD accelerators and design of heat exchangers, as provoked by Hari etal. [12].

. Non-Newtonian fluids are those for which the shear stress is not linearly proportional to the deformation rate. In other words, fluids that do not satisfy Newton's law of viscosity are known as non-Newtonian fluids. Blood, paints, ketchup, shampoo, mud etc., behave like non-Newtonian fluids. Williamson fluid is one of non-Newtonian fluids. The study of Williamson fluids for the boundary layer flow is of great interest because of its vast range of applications in different branches of science, technology and engineering, especially in nuclear and chemical industries, bio-engineering and geophysics. Considering these applications extensive range of scientific models has been established to simulate the flow actions of these non-Newtonian fluids.

Williamson [13] discussed the flow of pseudo plastic materials and presented a model equation to discuss the pseudo plastic fluids flow and verified the results experimentally. Nadeem et al. [14] presented the Williamson fluid flow past a stretching surface and found that, by increasing values of Williamson fluid parameter, the dimensionless velocity decreases. Heat transfer characteristics on non-Newtonian nanofluid flow over a stretching sheet were presented by Nadeem and Hussain [15]. Hayat and Hina [16] studied the impact of mass and heat transfer with flexible walls on Williamson fluid flow.

Recently, flows of boundary layer of Newtonian and non-Newtonian fluids have drawn considerable attention because of their significant applications in processing of metallurgical, phenomena of chemical engineering transport, molten polymers extrusion, plastic sheets and wrapping foils fabrication etc. Species, momentum and heat transport play a major role in such processes [17]. In this article, provides the review work of research paper of M. Krishnamurthy et al. [18] and extends the work for the impact of viscous dissipation on MHD Williamson nanofluid past the horizontally stretching sheet.

Manuscript published on 30 September 2019
* Correspondence Author
N. Manjula*, Department of Mathematics, Sreenidhi Institute of Science and Technology, Hyderabad, India.
Email: nagula_manju@yahoo.com
K. Govardhan, Department of Mathematics, GITAM University, Hyderabad, India.
Email: govardhan_kmtm@yahoo.co.in
MN Rajashekar, Department of Mathematics, JNTU College of Engineering Jagtial, India. Email: mnrs@jntuh.ac.in

II. MATHEMATICAL FORMULATIONS

Consider MHD boundary layer flow of incompressible Williamson nanofluid.

The flow is 2Dpast a stretching surface in a porous medium. Schematic diagram of a system under investigation is shown in the Figure 1.The plate is stretched along $x-$axeswith velocity$u = ax, (a > 0)$. Amagnetic field is applied along the $y-$direction. The temperature at surface isT_w, fluid velocity isU_w,C_w representsurfaceconcentration. Moreover, T_m denotes the melting surfacetemperature and T_∞denotes the free stream temperature of the nanofluid. The free stream temperature T_∞ is greater than the melting surface temperatureT_m.

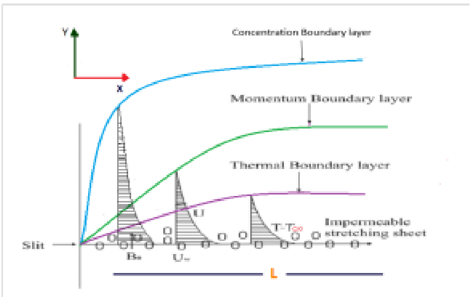

Figure 1: Geometry of the physical model.

Under the above constraints, the boundary layer equations are given as:

$$\frac{\partial u}{\partial x}+\frac{\partial v}{\partial x}=0 \qquad (1)$$

$$u\frac{\partial u}{\partial x}+v\frac{\partial v}{\partial y}=\nu\frac{\partial^2 u}{\partial y^2}+\sqrt{2}\nu\frac{\partial u}{\partial y}\frac{\partial^2 u}{\partial y^2}-\sigma\frac{B_0^2}{\rho}u-\frac{\nu}{k'}u \qquad (2)$$

$$u\frac{\partial T}{\partial x}+v\frac{\partial T}{\partial y}=\alpha_m\frac{\partial^2 T}{\partial y^2}-\frac{1}{(\rho c)_f}\frac{\partial q_r}{\partial y}+\tau\left(D_B\left(\frac{\partial T}{\partial y}\frac{\partial C}{\partial y}\right)+\frac{D_T}{T_\infty}\left(\frac{\partial T}{\partial y}\right)^2\right)+\frac{\nu}{(\rho c)_f}\left(\frac{\partial u}{\partial y}\right)^2 \qquad (3)$$

$$u\frac{\partial C}{\partial x}+v\frac{\partial C}{\partial y}=D_B\left(\frac{\partial C}{\partial y}\right)^2+\frac{D_T}{T_\infty}\left(\frac{\partial^2 T}{\partial y^2}\right)-k_0 \qquad (4)$$

The associated boundary conditions for the modeled problem:

$$\left.\begin{aligned} &u=U_w(x)=ax, T=T_m, C=C_w \text{ at } y=0,\\ &u=0, T\to T_\infty, C\to C_\infty \text{ as } y\to\infty,\\ &k\left(\frac{\partial T}{\partial y}\right)_{y=0}=\rho[\beta+c_s(T_m-T_0)]v(x,0).\end{aligned}\right\} \qquad (5)$$

where u and v denote the components of fluid velocity along x and y direction,respectively, T denotes the temperature of the nanofluid, $\rho$the nanofluid density,$\alpha_m$the thermal diffusivity of the nanofluid, ν the kinematic viscosity, D_B thecoefficient of Brownian diffusion, D_T thecoefficient of thermophoresis diffusion,$k'$the porous medium permeability, $(\rho c)_f$the heat capacity of the fluid and $(\rho c)_p$denotes the heat capacity of the nanoparticle.

III. NON-DIMENSIONAL FORM OF THE GOVERNING EQUATIONS:

The dimensional PDEs are converted into the non-dimensional form by similarity transformation. We introduce the following dimensionless similarity variable

$$\eta=y\sqrt{\frac{a}{\nu}}, \psi=\sqrt{a\nu}\,xf(\eta), \theta(\eta)=\frac{T-T_m}{T_\infty-T_m}\ ,\ \beta(\eta)=\frac{C-C_\infty}{C_w-C_\infty}\ . \qquad (6)$$

After using similarity transformation, the equations take the form

$$ff''-(f')^2+W_e f''f'''-(Q+k_p)f'+f'''=0 \qquad (7)$$

$$\frac{\left(1+\frac{4}{3}R\right)\theta''}{Pr}+f\theta'+Nb\theta'\beta'+Nt(\theta')^2+Ec(f'')^2=0 \qquad (8)$$

$$\beta''+Lef\beta'+\frac{Nt}{Nb}\theta''-Le\gamma\beta=0 \qquad (9)$$

The relevant boundary conditions are:

$$\left.\begin{aligned} &f'(0)=1, \Pr f(\theta)+M\,\theta'(0)=0, \theta(0)=0,\\ &\beta(0)=0, \text{at } \eta=0,\\ &f'(\infty)\to 0, \theta(\infty)\to 1, \beta(\infty)\to 1 \text{as } \eta\to\infty\end{aligned}\right\} \qquad (10)$$

The physical constraints appeared in Eq. (7) to Eq. (10), we represents

$$Pr=\frac{\nu}{\alpha}, R=\frac{-4T_\infty^3\sigma^*}{3k^*k}, k_p=\frac{\nu}{k'a}, W_e=\gamma x\sqrt{\frac{2a^3}{\nu}},$$

$$\gamma=\frac{k_0U(C_\infty-C_w)}{\nu}, Nt=\frac{\tau D_T(T_w-T_m)}{\nu T_\infty}, Q=\frac{\sigma B_0^2}{\rho a}, Le=\frac{\nu}{D_B},$$

$$Nb=\frac{\tau D_B(C_\infty-C_m)}{\nu}, Ec=\frac{u_w^2}{\rho_f(T_w-T_m)}.$$

where Pr is the representation of the Prandtl number,Rrepresents the thermal radiation parameter,k_p the permeability parameter, W_e the non-Newtonian Williamson parameter,γ the chemical reaction parameter,Nt stands for thermophoresis parameter, Q the magnetic parameter, Le the Lewis number,Brownian motion parameter is denoted by Nb and Ec the Eckert number.

Nusselt number, Sherwood number and the skin friction coefficients are expressed as:

$$Nu_x=\frac{xq_w}{k((T_\infty-T_m)}, Sh_x=\frac{xq_m}{D_B((C_\infty-C_w)}\text{and } C_f=\frac{\tau_w}{\rho U_w^2}, \qquad (11)$$

where, $\tau_w$is the shear stress along the stretching surface, $q_w$is the heat fluxfrom the stretching surface and q_m is the wall mass flux, are given as:

$$q_w=-k\left(\frac{\partial T}{\partial y}\right)_{y=0}, q_m=-D_B\left(\frac{\partial C}{\partial y}\right)_{y=0}, \tau_w=\mu\left(\frac{\partial u}{\partial y}+\right.$$

Γ2∂u∂y2y=0, (12)

Using the dimensionless variables, we get

$$\frac{Nu_x}{\sqrt{R_x}}=-\theta'(0), \frac{Sh_x}{\sqrt{R_x}}=-\beta'(0)\ ,$$

$$C_f\sqrt{R_x}=-\ f''(0)+\frac{\lambda}{2}f''(0)^2 \qquad (13)$$

where Re_x denotes the Reynolds number and is expressed as $Re_x=\frac{xU_w(x)}{\nu}$.

IV. NUMERICAL SOLUTION

The system of higher order ODE is converted into first order ODEs. The prescribed boundary conditions are also converted into first order system of ordinary differential equations (ODEs).

The first order system of ordinary differential equations including the related boundary conditions is solved numerically using Fortran Language.

$$f''' = \frac{1}{1+\lambda f''}(-ff'' + (f')^2 + (Q + k_p)f'$$

$$\theta'' = \frac{3Pr}{3+4R}(-f\theta' - Nb\theta'\beta' - Nt(\theta')^2 - Ec(f'')^2$$

$$\beta'' = -Lef\beta' - \frac{Nt}{Nb}\theta'' + Le\gamma\beta$$

By using the following notations,

$$\left.\begin{array}{l} f = y_1, f' = y_1' = y_2, f'' = y_2' = y_3, \\ \theta = y_4, \theta' = y_4' = y_5, \theta'' = y_5', \\ \beta = y_6, \beta' = y_6' = y_7, \beta'' = y_7'. \end{array}\right\} \quad (14)$$

The system of first order ODEs are:

$$y_1' = y_2, \qquad y_1(0) = r \quad (15)$$

$$y_2' = y_3, \qquad y_2(0) = 1 \quad (16)$$

$$y_3' = \frac{1}{1+\lambda y_3}(-y_1y_3 + (y_2)^2 + (Q + k_p)y_2$$

$$y_3(0) = s \quad (17)$$

$$y_4' = y_5 \qquad y_4(0) = 0 \quad (18)$$

$$y_5' = -\frac{3Pr}{3+4R}(y_1y_5 + Nby_5y_7 + Nty_5^2 + Ecy_3^2)$$

$$y_5(0) = -\frac{Pr}{M} \quad (19)$$

$$y_6' = y_7 \qquad y_6(0) = 0 \quad (20)$$

$$y_7' = -Ley_1y_7 - \frac{Nt}{Nb}y_5' + Le\gamma y_6,\ y_7(0) = t \quad (21)$$

To solve the above system of equations, the unbounded domain $[0, \eta_\infty]$ is restricted to bounded domain $[0, \eta_e]$ where $\eta_e = 5$.This is since increasing the value of $\eta_e$beyond 5 gives negligible variation in the numerical results. In the modeled problem,$r^{(0)}, s^{(0)}, t^{(0)}$are initial guesses which are required to solve the above first order system of ordinary differential equations with fourth order Adams-Bashforth Moulton Method. Newton iterative scheme is used to refine those initial guesses. The iterative process is repeated until the following conditions is met.

$$max(|y_2(\eta_\infty)|, |y_4(\eta_\infty) - 1|, |y_6(\eta_\infty) - 1|) < 10^{-3}$$

V.RESULTS AND DISCUSSION

The main purpose of this part is to analyze velocity, temperature, and concentration profiles. Table 1is prepared to study the impact of various parameters on the $-\theta'(0)$ and$-\beta'(0)$. From this table, we can see that by increasing the values of permeability parameter, non-Newtonian Williamson parameter, chemical reaction parameter, Eckert number, $-\theta'(0)$ decreasing whereas the $-\beta'(0)$ is increased. By increasing the dimensionless melting parameter $-\theta'(0)$ increasing and Sherwood number is decreased.

The impact of dimensionless melting parameter on velocity profile $f'(\eta)$ and dimensionless temperature profile $\theta(\eta)$ is shown in Figure 2and 3respectively.The graphical demonstration shows that for the increasing values of dimensionless melting parameter, the velocity profile and thickness of the boundary layerincreases slightly and the temperature distribution decreases. It is found that an increase in the dimensionless melting parameter increases the melting intensity, which acts as boundary condition at the stretching surface and tends to make the boundary layer thicker.

Impact of Radiation parameter is shown in Figure 4. It is seen that for gradually enhancing values of R energy profile also decreased. Due to increase in thermalRadiation parameter more heat to fluid produces that enhance the energy filedwith chemical effect on the melting surface. Figure 5also represents that concentration profile is increased for increasing values of radiation parameter.

From the figure 6, it is observed that by increasing values of Lewis number temperature near the surface of plate decreases and away from the surface of plate increases. Figure7 reflects the effect of Lewis number on concentration profile. Lewis number can be defined as the ratio of thermal diffusion to the molecular diffusion. It is convenient of help us find the relation between mass and heat transfer coefficient. By increasing Lewis number, the concentration profile becomes steeper.

Figures 8 and 9 demonstrate the influence of the magnetic parameter on the dimensionless profile of velocity distribution $f'(\eta)$and dimensionless profile of temperature distribution $\theta(\eta)$, respectively. From these figures, with increasing values of the magnetic parameter, profile of velocity decreases. It is also observed that temperature distribution $\theta(\eta)$ shows increasing effects as the magnetic parameter increases. The reason beyond this electrically conducting fluid produces a resistive force known as Lorentz force, which opposes the flow and tends to make the fluid motion slowdown in the boundary layer and therefore reduces the profile of velocity whereas its temperature $\theta(\eta)$ increases with the increase in magnetic parameter.

Table 1: $-\theta'(0)$ and $-\beta'(0)$ for different parameters.

k_p	M	W_e	γ	Ec	$-\theta'(0)$	$-\beta'(0)$
0.5	0.5	0.2	0.01	0.2	-2.240853000	0.524976800
1.0					-2.166060000	0.549167900
1.5					-2.098345000	0.574106300
2.0					-2.037475000	0.600233300
	1.0				-1.363586000	0.331753700
	1.5				-1.044776000	0.225277800
	2.0				-0.856633100	0.172704300
	2.5				-0.732235500	0.143191300
		0.0			-2.082783000	0.574948000
		0.05			-2.072699000	0.579855900
		0.1			-2.061879000	0.585522400
		0.2			-2.037475000	0.600233300
			0.0		-2.094427000	0.595451500
			0.1		-1.770716000	0.638036800
			0.2		-1.679036000	0.640612900
			0.3		-1.650183000	0.625154200
				0.0	-1.736491000	0.276181700
				0.3	-2.182688000	0.741150400
				0.7	-2.743267000	1.193489000
				1.0	-3.164277000	1.442901000

The impact of Pr on the profile of temperature field in the presence of meltingparameter is displayed in Figure 10. From figure, we deduce that by increasingthe values of Prandtl number, temperature profile increases. This is because thelarger values of Prandtl number possess smaller thermal diffusivity and smaller Prandtl number have stronger thermal diffusivity.

The impact of thermophoresis parameter on the dimensionless profile of temperature distribution $\theta(\eta)$ and dimensionless profile of concentration distribution $\beta(\eta)$are presented respectively in Figures 11and 12. It is clear, from these figuresprofile of temperature and their associative thickness of thermal boundary layer ofthe thermal field increase with the increasing values of thermophoresis parameter.It is also noticed that for varying values of Nt concentration profile $\beta(\eta)$ and related thickness of boundary layer decreases.

Figures 13and 14 depict that by increasing Brownian motion parameter, temperature profile and thickness of boundary layer increases slightly whereas concentration profile decreases significantly.

Figures 15and 16indicate the influence of the permeability parameter on the dimensionless profile of velocity distribution $f'(\eta)$ and dimensionless profile of thetemperature produces a resistive force, that has a tendency to slow down the fluid motion. It is observed that resistance decreases in the fluid motion by increasing values of the permeability parameter. Therefore, it is concluded that velocity profile $f'(\eta)$ and temperature profile $\theta(\eta)$ decreases by increasing values of permeability parameter.

From Figures 17and 18, we observe the effect of non-Newtonian Williamson parameter on the velocity and temperature profiles respectively. It is observed that the velocity profile and thickness of boundary layer decrease by increasing values ofW_e. It is also observed that the profile of temperature and thickness of thermal boundary layer decreases.

The effects of chemical reaction coefficient for concentration profile are observed in the Figure 19, which show that by increasing γ , the concentration profile decreases, and it also decreases inthe thickness of concentration.

In Figure 20, it indicates that increasing the value of Eckert number Ec has the enhancing effect on temperature profile and increases the thermal boundary layer thickness in the flow field. The temperature increases due to increasing the Eckert numberEc that generates heat in fluid.

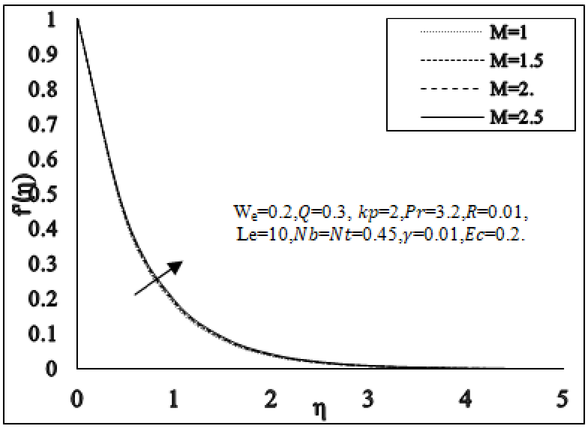

Figure 2: Impact of M on the Velocity Profile

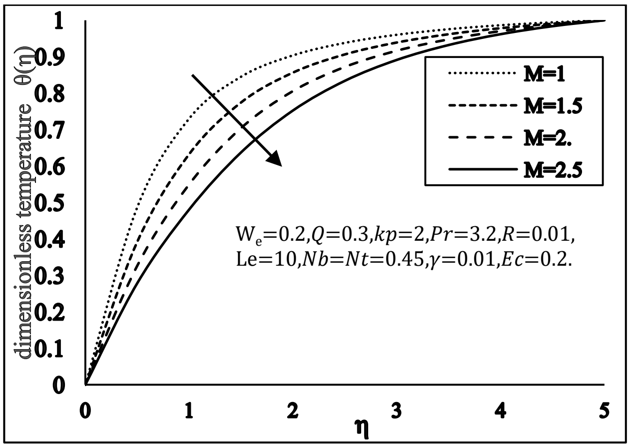

Figure 3: Impact of M on the Temperature Field

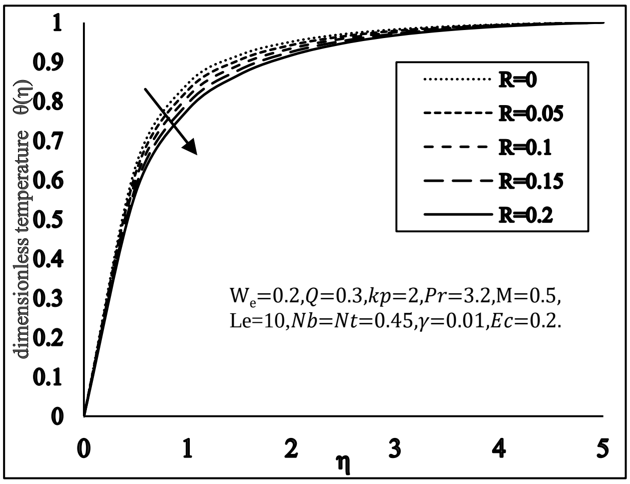

Figure 4: Impact of R on the Dimensionless Temperature

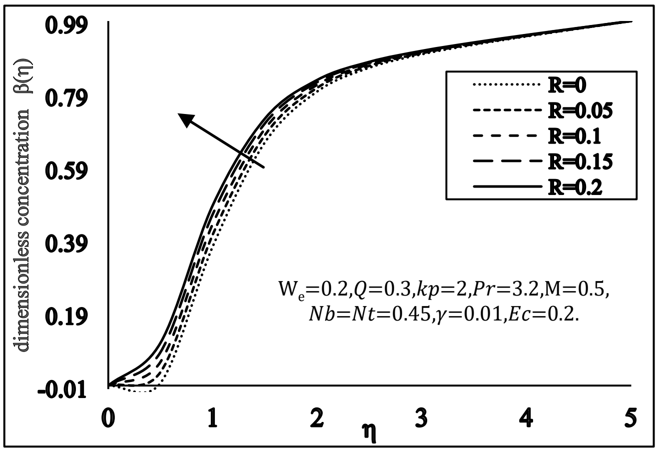

Figure 5: Impact of R on the dimensionless concentration

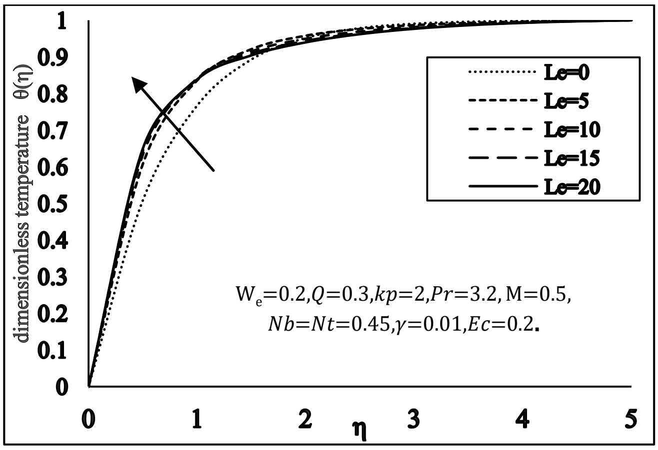

Figure 6: Impact of Leon the dimensionless temperature

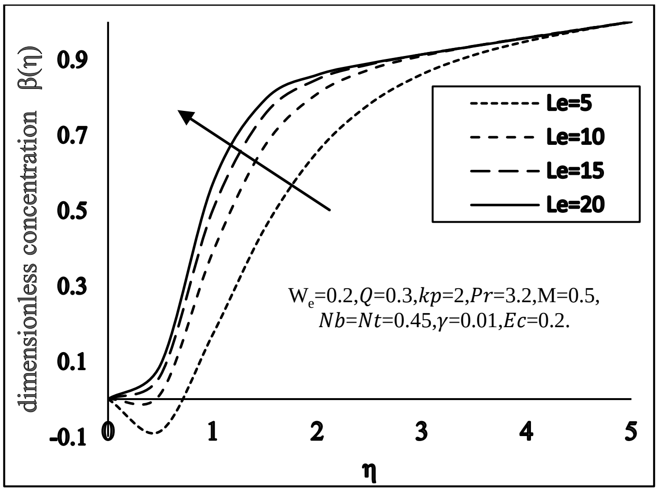

Figure 7: Impact of *L*eon the dimensionless concentration

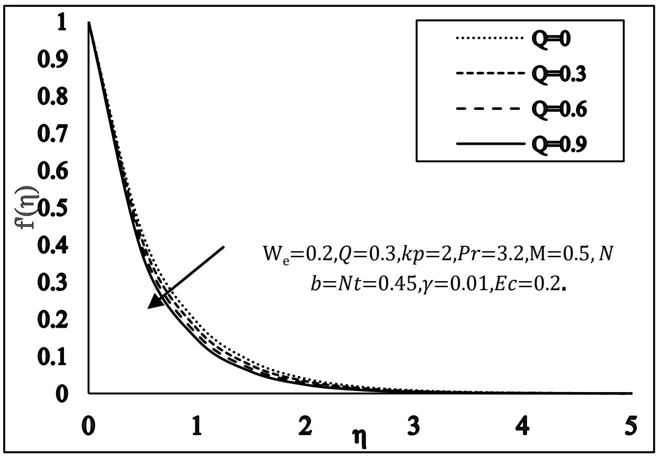

Figure 8: Impact of Q on the Velocity Field

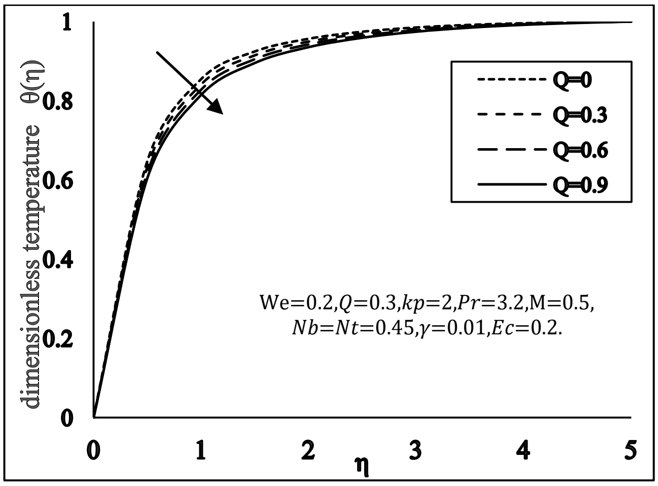

Figure 9: Impact of Q on the Temperature Profile

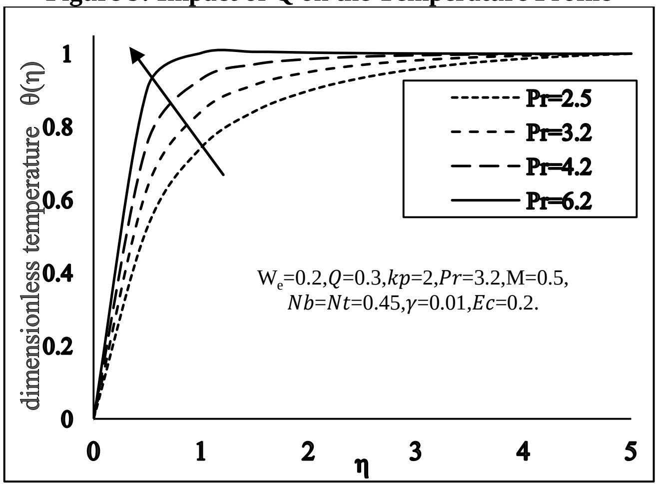

Figure 10: Impact of Pr on the dimensionless temperature

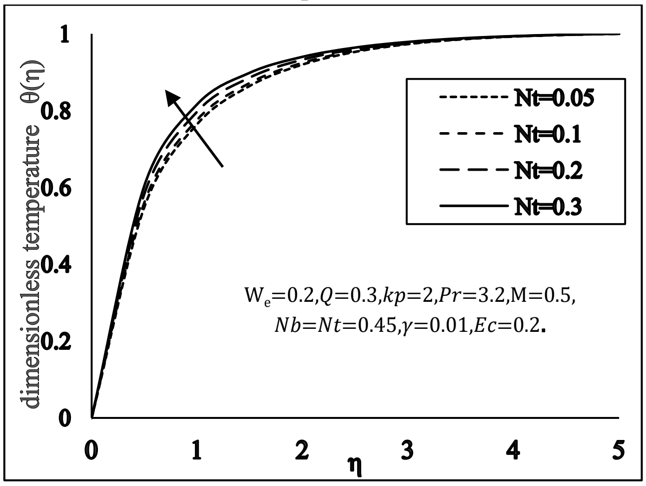

Figure 11: Impact of Nton the dimensionless temperature

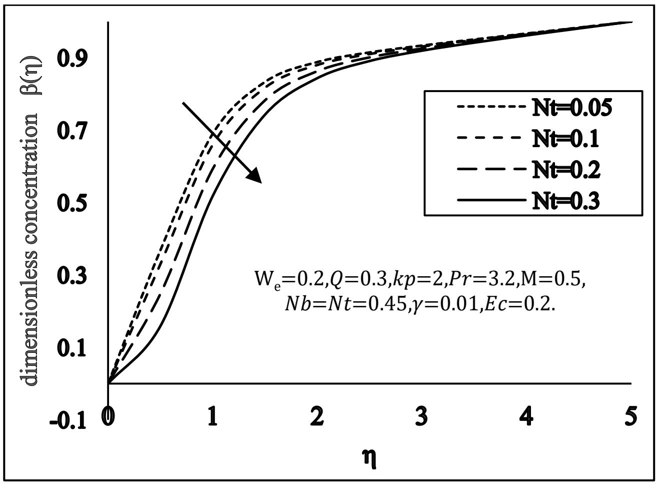

Figure 12: Impact of Nton the dimensionless concentration

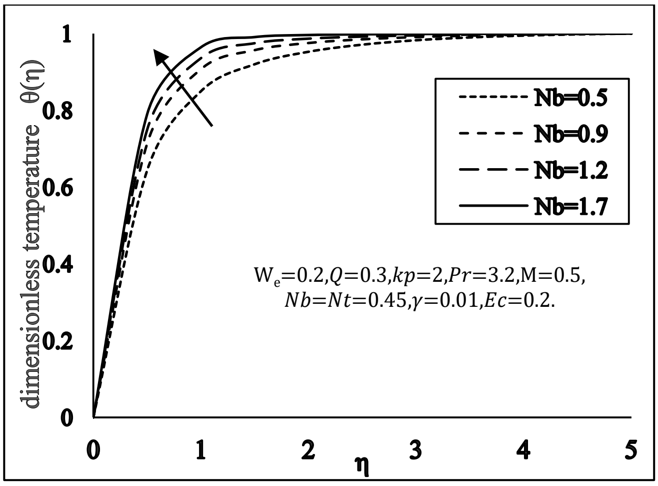

Figure 13: Impact of Nbon the dimensionless temperature

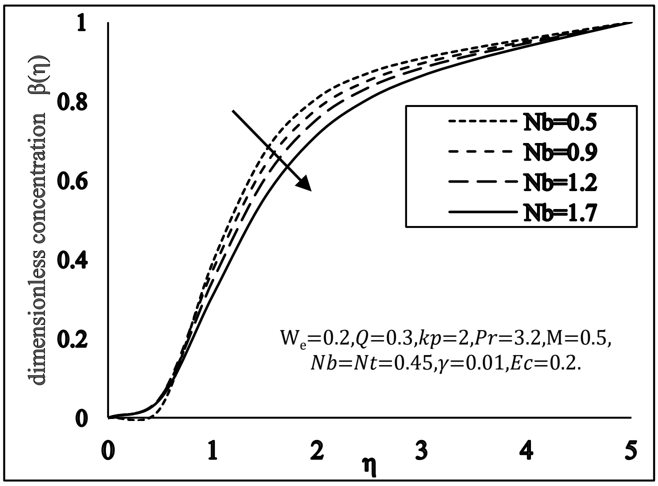

Figure 14: Impact of Nbon the dimensionless concentration

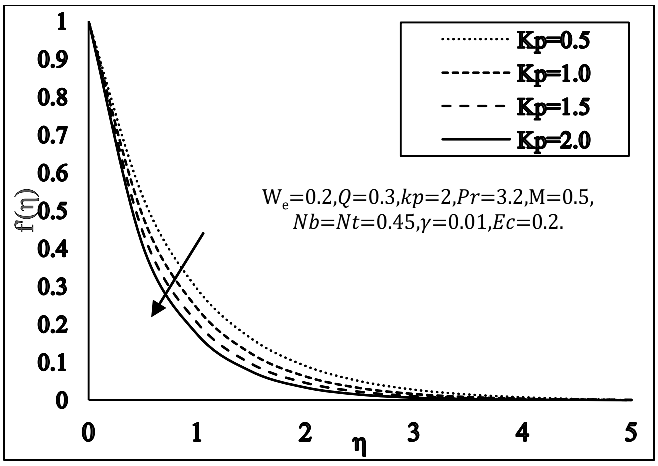

Figure 15: Impact of k_p on the dimensionless velocity

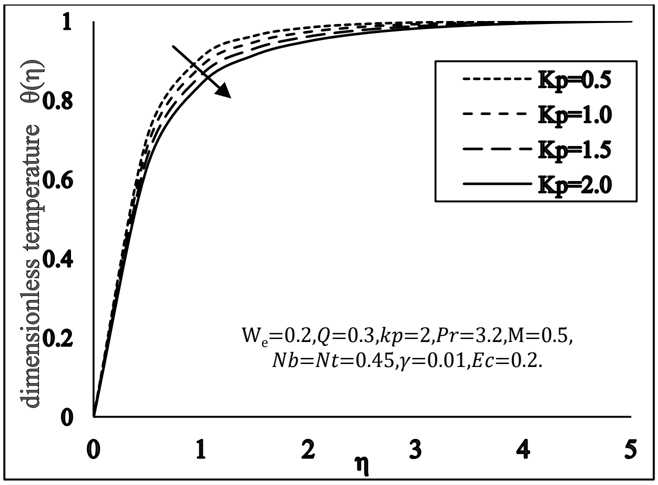

Figure 16: Impact of k_p on the dimensionless temperature

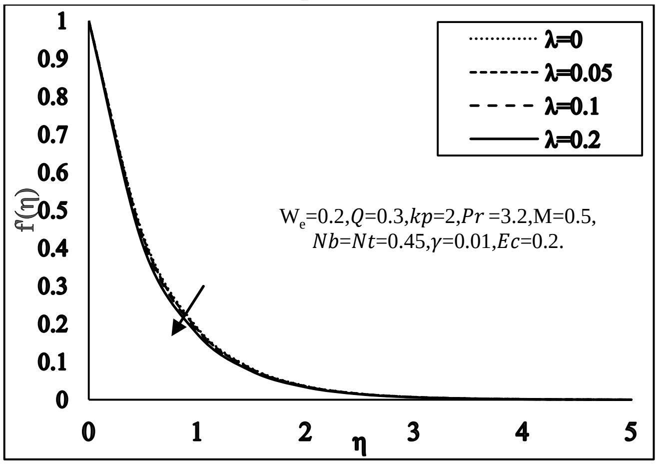

Figure 17: Impact of λ on the dimensionless velocity

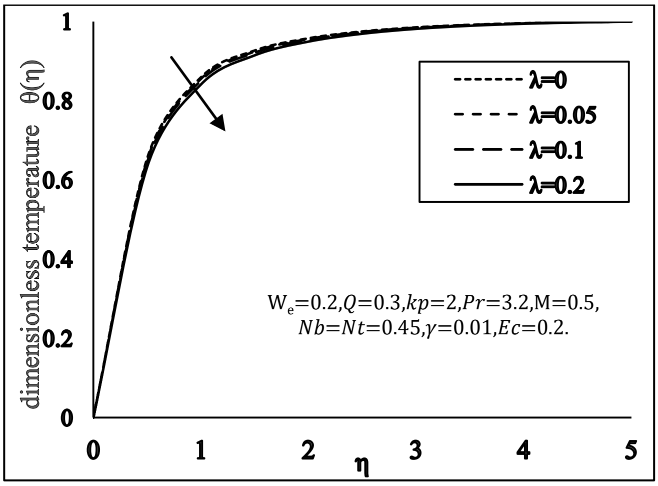

Figure 18: Impact of λ on the dimensionless temperature

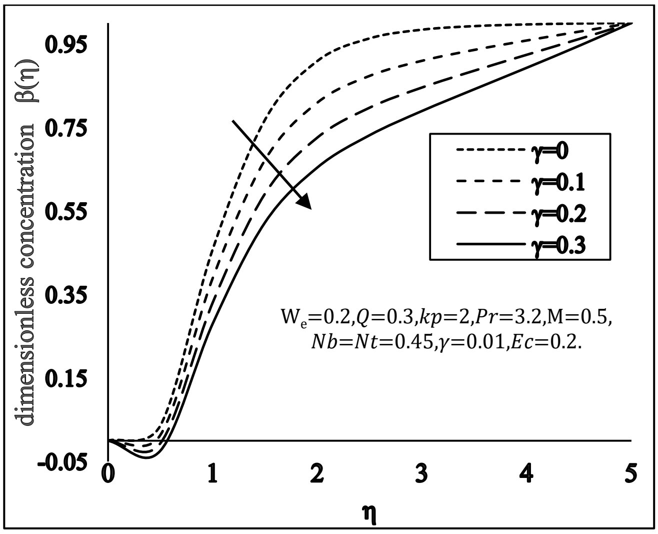

Figure 19: Impact of γ on the dimensionless concentration

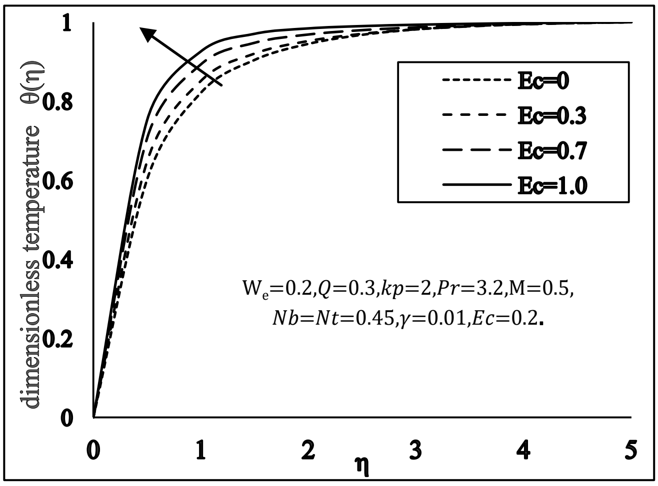

Figure 20: Impact of Ec on dimensionless temperature

VI. CONCLUSION

The concluding remarks and the important findings of the investigation from graphical representation are listed below:

- It is reported that for enhancing values of the radiation parameter and Magnetic parameter, temperature increases whereas the concentration decreases.
- Increases the velocity profile decreases gradually and increasing effects on the temperature.
- Decrement in temperature profile is observed for increasing values of the Prandtl number.
- For increasing the Brownian parameter, the temperature profile increases and the concentration profile.
- Velocity field and Temperature field both are decreases by enlarging permeability parameterk_p.
- An increase in non-Newtonian Williamson parameter sources decrease in the velocity profile and similar effects on temperature.
- By increasing the thermophoresis parameter Nt , momentum increases, and concentration decreases.

REFERENCES

1. G. B. Meir, "Basic of fluid mechanics," M. Genick. Chicago, 2013.
2. B. Sakiadis, "Boundary layer behavior on continuous solid surfaces," J.AIChE, vol. 7, no. 1, pp. 26-28, 1961
3. L. Crane, "Flow past a stretching plate," Zeitschrift fur angewandteMathematik und Physik, vol. 21, no. 4, pp. 645-647, 1970.
4. S. Shehzad, Z. Abdullah, F. Abbasi, T. Hayat, and A. Alsaedi, "Magnetic field effect in three-dimensional flow of an oldroyd-B nanofluid over a radiative surface," J. Magn. Magn. Mater, vol. 399, pp. 97-108, 2016.
5. L. Zheng, J. Niu, X. Zhang, and L. Ma, "Dual solutions for flow and radiative heat transfer of a micropolar fluid over stretching/shrinking sheet," Int. J. Heat Mass Transf., vol. 55, no. 25, pp. 7577-7586, 2012.
6. B. Gireesha, A. Chamkha, S. Manjunatha, and C. Bagewadi, "Mixed convective flow of a dusty fluid over a vertical stretching sheet with non-uniform heat source/sink and radiation," Int. J. Num. Meth. Heat Fluid Flow, vol. 23, no. 4, pp. 598-612, 2013.
7. H. Alfven, "Existence of electromagnetic-hydrodynamic waves," Nature, vol. 150, no. 3805, pp. 405-406, 1942.
8. I. Mbeledogu and A. Ogulu, "Heat and mass transfer of an unsteady MHD natural convection flow of a rotating fluid past a vertical porous at plate in the presence of radiative heat transfer," Int. J. Heat Mass Transf., vol. 50, no. 9, pp. 1902-1908, 2007.
9. P. Kesavaiah, D. C. Satyanarayana and S. Venkataramana, "Effects of the chemical reaction and radiation absorption on an unsteady MHD convective heat and mass transfer flow past a semi-infinite vertical permeable moving plate embedded in a porous medium with heat source and suction," Int. J. Appl. Math. Mech., vol. 7, no. 1, pp. 52-69, 2011.
10. T. Hayat, S. Asad, M. Mustafa, and A. Alsaedi, "MHD stagnation-point flow of Jeffrey fluid over a convectively heated stretching sheet," Comput. Fluids, vol. 108, pp. 179-185, 2015.
11. M. Mustafa, J. Khan, T. Hayat, and A. Alsaedi, "Sakiadisflow of Maxwell fluid considering magnetic field and convective boundary conditions," AIP Adv., vol. 5, no. 2, pp. 027106, 2015.
12. N. Hari, M. Sivasankaran, S. Bhuvaneswari, and Z. Siri, "Effects of chemical reaction on MHD mixed convection stagnation point flow toward a vertical plate in a porous medium with radiation and heat generation," J. Phys., vol. 662, no. 1, p. 012014, 2015.
13. R. V. Williamson, "The flow of pseudo plastic materials," Ind. Eng. Ch., vol. 21, no. 11, pp. 1108-1111, 1929.
14. S. Nadeem, S. Hussain, and C. Lee, "Flow of a Williamson fluid over a stretching sheet," Braz. J. Chem. Eng., vol. 30, no. 3, pp. 619-625, 2013.
15. S. Nadeem and S. Hussain, "Flow and heat transfer analysis of Williamson nanofluid," Appl. Nanosci., vol. 4, no. 8, pp. 1005-1012, 2014.
16. T. Hayat and S. Hina, "Effects of heat and mass transfer on peristaltic flow of Williamson fluid in a non-uniform channel with slip conditions," Int. J.Num. Methods in Fluids, vol. 67, no. 11, pp. 1590-1604, 2011
17. V. Kumaran and G. Ramanaiah, "A note on the flow over a stretching sheet,"Acta Mecca, vol. 116, no. 1, pp. 229-233, 1996.
18. M. Krishnamurthy, B. Prasannakumara, B. Gireesha, and R. Gorla, "Effect of chemical reaction on MHD boundary layer flow and melting heat transfer of Williamson nanofluid in porous medium," Eng. Sci. Technol. Int. J., vol. 19, no. 1, pp. 53-61, 2016.

AUTHORS PROFILE

N. Manjula, Department of Mathematics, Sreenidhi Institute of Science and Technology, Hyderabad, Telangana State, India.

K.Govardhan, Department of Mathematics, GITAM University, Hyderabad, Telangana State, India.

M.N.Rajashekar, Department of Mathematics, JNTU College of Engineering Jagtial, Telangana State, India.